Monatsh Chem 139, 1417–1422 (2008)
DOI 10.1007/s00706-008-0959-4
Printed in The Netherlands

**Monatshefte für Chemie
Chemical Monthly**

Effect of pulegone and pulegone oxide on the corrosion of steel in 1 *M* HCl

Zaid Faska[1], Aicha Bellioua[1], Mohamed Bouklah[2], Lhou Majidi[1], Rachid Fihi[1],
Abdelahamid Bouyanzer[2], Belkheir Hammouti[2]

[1] Laboratoire des substances naturelles & synthèse et dynamique moléculaire, Faculté des Sciences et Techniques, Errachidia, Morocco
[2] Laboratoire de chimie Appliquée & Environnement, Faculté des Sciences, Oujda, Morocco

Received 26 September 2007; Accepted 5 May 2008; Published online 31 July 2008

Abstract The inhibitive action of pulegone and pulegone oxide toward acid corrosion of steel in molar hydrochloric acid was studied by weight loss measurements, potentiodynamic polarization, and impedance spectroscopy (EIS) methods. The pulegone is extracted starting from oil of Pennyroyal Mint (*Mentha pulegium*). The natural compound was found to delay the corrosion rate. The pulegone oxide is prepared by oxidation of pulegone. The inhibition efficiency was found to increase with the inhibitor content to attain 81 and 75% at 5 g dm^{-3} for pulegone and pulegone oxide. The increase in temperature leads to an increase in the inhibition efficiency of the natural compared.

Keywords Steel; Corrosion; Inhibition; Pulegone; Pulegone oxide; Adsorption.

Introduction

The use of inhibitors becomes more and more popular to prevent corrosion of metals in many fields such as cooling systems, refinery units, chemicals, oil and gas production units, boiler, *etc*. The role of inhibitors added in low concentrations to corrosive media, is to decrease or stop the reaction of the metal with the medium Inhibitors act by adsorption of ions or molecules onto the metal surface. They generally reduce the corrosion rate by blocking of the anodic and/or cathodic reaction, or by decreasing the diffusion rate for reactants to the surface of the metal or decreasing the electrical resistance of the metal surface [1–3].

Several considerations have to be taken into account when choosing an inhibitor:

- Cost of the inhibitor can be sometimes very high when the material involved is expensive or when the amount needed is huge.
- Toxicity of the inhibitor can cause jeopardizing effects on human beings and other living species.
- Availability of the inhibitor will determine its selection and if the availability is low, the inhibitor becomes often expensive.
- Environmental friendliness.

Owing to increasing ecological awareness and strict environmental regulations and the need to develop environmentally friendly processes, attention is now focused on the development of substitute non toxic alternatives to inorganic inhibitors already used. Natural products extracted from plant sources, as well as some non toxic organic compounds, which contain polar functions with nitrogen, oxygen, and/or sulfur in conjugated systems in their molecules [3–5], have been effectively used as inhibitors in

Correspondence: Belkheir Hammouti, Laboratoire de chimie Appliquée & Environnement, Faculté des Sciences, B.P. 717, 60000 Oujda, Morocco. E-mail: hammoutib@yahoo.fr

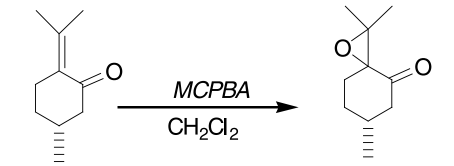

Pulegone Pulegone oxide

Scheme 1

many corrosion systems. These organic compounds are either synthesized or extracted from aromatic herbs, spices, and medicinal plants. These advantages have incited us to draw a large part of our laboratory program to examine extracts of natural substances as corrosion inhibitors [6–10]. These have been found to be very efficient corrosion inhibitors for iron and steel in acidic media. Jojoba and bgugaine offer an efficiency of 100% for the protection of steel in acidic media [7, 11].

The encouraging results obtained by the natural products on one hand and by Pennyroyal Mint oil [12] on the other hand encouraged us to test the existent pure products of these extracts. The pulegone and its synthesized oxide (Scheme 1) are tested on the corrosion of steel in acid solution. Pennyroyal oil from *Mentha pulegium* has been widely used as fragrance component, a flavoring agent, and also as herbal medicine to terminate pregnancy [13]. Pulegone is the principal constituent of this oil. Pulegone is also present in peppermint and mint oil, obtained from *Mentha piperita*, *Mentha arvensis* [14], and *Ziziphora tenuior* [15]. In this paper, gravimetric and electrochemical techniques are applied to study the ability of pulegone (*P*) and pulegone oxide (*PO*) to inhibit the corrosion of steel in 1 *M* HCl. The effect of temperature is also studied.

Results and discussion

Steel samples were immersed for 6 h at 298 K in aerated 1 *M* HCl at various contents of *P* and *PO*. Table 1 shows the variation of the corrosion rate of steel with the inhibitor concentration. The calculated inhibition efficiencies of the compounds *P* and *PO* are also given in Table 1. The natural products present an inhibitive effect (IE_W) on the corrosion of steel in acid solution. IE_W increases with natural product content to attain 81 and 75% at 5 g dm^{-3} for *P* and *PO*. We may conclude that *P* and *PO* are good inhibitors of steel corrosion in 1 *M* HCl.

Table 1 Steel weight loss data and inhibitor efficiency of *P* and *PO* at 298 K after 6 h

Concentration / g dm^{-3}	$W(P)$ / mg cm^{-2} h^{-1}	IE_W/ %	$W(PO)$ / mg cm^{-2} h^{-1}	IE_W/ %
0	0.2762	–	0.2762	–
0.25	0.1933	30	0.1905	31
0.5	0.1408	49	0.1657	40
1	0.0994	64	0.1381	50
2	0.0828	70	0.0994	64
2.5	0.0773	72	0.0939	66
3	0.0746	73	0.0911	67
4	0.0616	78	0.0801	71
5	0.0529	81	0.0690	75

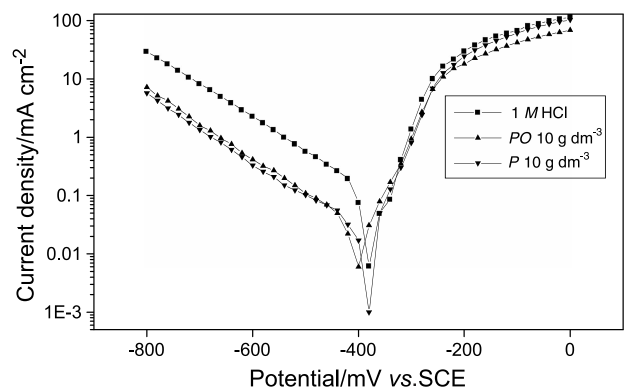

Fig. 1 Polarization curves of steel in 1 *M* HCl without and with 10 g dm^{-3}

The lower efficiency of *PO* is probably due to its instability in acidic media. This result is also confirmed by the polarization study (Fig. 1). Values of associated electrochemical parameters such as corrosion potential (E_{corr}), corrosion current density (i_{corr}), and the calculated IE_i are given in Table 2. The effect of compounds studied is marked by cathodic action.

The polarization curves for the steel electrode in 1 *M* HCl at different concentrations of *P* were recorded and Table 3 regroups the electrochemical

Table 2 Electrochemical parameters of steel in 1 *M* HCl without and with 10 g dm^{-3} of *P* and *PO*: corrosion potential (E_{corr}), corrosion current density (i_{corr}), and calculated inhibitor efficiency (IE_i)

Sample	E_{corr}/mV SCE^{-1}	i_{corr}/μA cm^{-2}	IE_i/%
Blank	−396	78	–
P	−417	12	85
PO	−405	18	77

Table 3 Electrochemical parameters of steel in 1 *M* HCl at various concentrations of *P*: corrosion potential (E_{corr}), anodic and cathodic *Tafel* slopes, β_a and β_c, corrosion current density (i_{corr}), and calculated inhibitor efficiency (IE_i)

c/g dm^{-3}	E_{corr}/mV SCE^{-1}	β_c/mV dec^{-1}	β_a/mV dec^{-1}	i_{corr}/ μA cm^{-2}	IE_i/ %
Blank	−396	176	82	78	–
0.25	−397	176	90	62	21
0.5	−397	190	82	44	44
2	−401	193	79	25	68
3	−398	194	86	23	71
5	−412	175	86	16	80
10	−417	163	80	12	85

Table 4 Electrochemical parameters (charge transfer resistance, R_t, double layer capacitance, C_{dl}, and frequency values, f_{max}) of steel in 1*M* HCl + *P* at various concentrations and the corresponding inhibition efficiency (IE_R)

c/g dm^{-3}	$R_t/\Omega \cdot$ cm^{-2}	f_{max}/Hz	C_{dl}/μF cm^{-2}	IE_R/%
Blank	120	99.7	83.58	–
0.25	152	99.4	66.18	21
0.5	220	94.5	48.10	45
2	326	100	30.42	63
3	400	101	24.56	70
5	548	92	19.83	78
10	722	95	14.57	83

data. The addition of *P* leads to a decrease in the cathodic current densities. The cathodic portions give rise to *Tafel* lines indicating that the hydrogen evolution reaction is activation controlled. The addition of the inhibitor to the corrosive solution does not modify the cathodic *Tafel* slope β_c and thus the mechanism of the processes is not affected. The free corrosion potential determined after 30 min of immersion does not change in the presence of the inhibitor. The polarization curves for steel in HCl solution show that the presence of the compounds is of cathodic nature. This phenomenon is more pronounced with the concentration of the inhibitor. IE_i values increase with the concentration of inhibitor and it attains 85% at 10 g dm^{-3}.

Nyquist plots of steel in inhibited and uninhibited acidic solutions containing various concentrations of *P* are shown in Fig. 2. The charge transfer resistance, R_t, the double layer capacitance, C_{dl}, and the frequency, f_{max}, values are given in Table 4. The locus

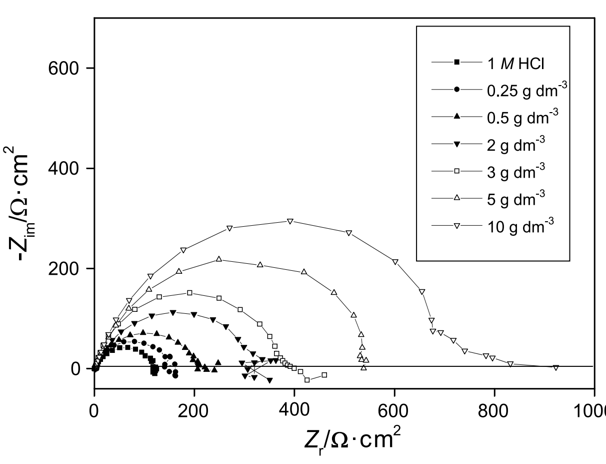

Fig. 2 *Nyquist* plots of steel in 1 *M* HCl containing various concentrations of *P*

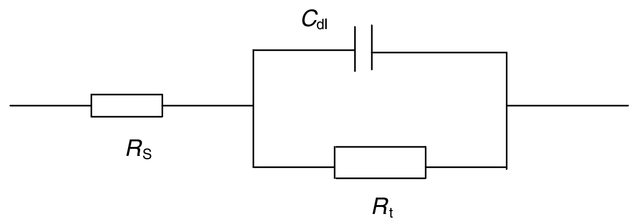

Fig. 3 Equivalent circuit used in the modeling of the EIS data

of *Nyquist* plots looks like one part of a semicircle. The equivalent circuit model used for this system is as that previously reported in Ref. [16] and is shown in Fig. 3. The semicircles obtained for the impedance diagrams indicate that the corrosion of steel is controlled by a charge transfer process. The charge transfer resistance (R_t) increases with the inhibitor concentration. Also, the double layer capacitance (C_{dl}) decreases with increase in the concentration of the inhibitor. This decrease is due to the adsorption of the inhibitor at the metal surface causing a change of the double layer structure [17]. When comparing the inhibition efficiencies (IE_W, IE_i, IE_R) obtained in this study by different techniques, it can be concluded that there is a fair agreement between the results.

The effect of temperature on the corrosion rate of steel in 1 *M* HCl containing inhibitor at a maximal concentration is studied in the temperature range of 303–333 K using weight loss measurements. The corresponding results are summarised in Table 5.

The increase in corrosion rate is more pronounced with the rise of temperature for the uninhibited acid solution. The presence of the inhibitor leads to a decrease of the corrosion rate. *IE* depends upon the temperature and increases with it. The following re-

Table 5 Effect of temperature on the steel corrosion in the absence and presence of *P* and *PO* after 2 h

Temperature/K	$\frac{W(\text{blank})}{\text{mg cm}^{-2}\,\text{h}^{-1}}$	$\frac{W(3\,\text{g dm}^{-3}\,P)}{\text{mg cm}^{-2}\,\text{h}^{-1}}$	IE_W/%	$\frac{W(5\,\text{g dm}^{-3}\,PO)}{\text{mg cm}^{-2}\,\text{h}^{-1}}$	IE_W/%
303	0.3280	0.1476	55	0.1804	45
313	0.7872	0.2912	63	0.3936	50
323	3.7064	0.8895	76	1.2231	67
333	5.3191	1.0638	80	1.5425	71

lation allows to determine the apparent activation energy:

$$W_{\text{corr}} = k \exp\left(\frac{E_a}{RT}\right) \quad (1)$$

where W_{corr} is the corrosion rate of steel and E_a is the activation energy.

ΔH_a and ΔS_a are calculated from the transition state according to the following equation [18]:

$$W_{\text{corr}} = \frac{RT}{Nh} \exp\left(\frac{\Delta S_a^*}{R}\right) \exp\left(-\frac{\Delta H_a^*}{RT}\right) \quad (2)$$

where R is the universal gas constant, h the *Planck*'s constant, N the *Avogadro*'s number, ΔS_a^* the entropy of activation, ΔH_a^* the enthalpy of activation, and T the absolute temperature. Figure 4 gives the variation of W_{corr}/T as function of $1/T$. ΔH_a^* and ΔS_a^* are evaluated from Fig. 4 and are given in Table 6.

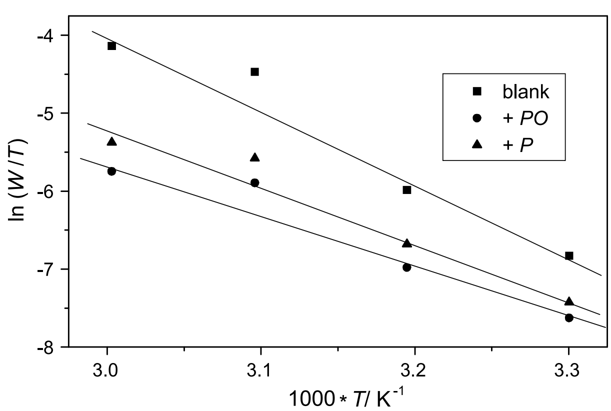

Fig. 4 Variation of ln (W/T) against T^{-1} for both the blank and the solution of inhibitor

Activation energies are calculated from the slopes of the *Arrhenius* lines (Fig. 5). Values obtained for E_a are 83.4, 63.8, and 59.3 kJ mol^{-1} in the absence of inhibitor and presence of *P* and *PO*. We note that the activation energy changes slightly in the presence of inhibitor. Furthermore, the increase of *IE* is explained by *Ammar* and *El Khorafi* [19] as chemisorption of inhibitor molecules on the steel surface. The lower value of E_a of the corrosion process in an inhibitor's presence when compared to that in its absence is attributed to its chemisorption [20, 21]. Recent works show that these inhibitors (terpenes) do not exceed 90% [2, 12, 22] but with sesquiterpenes (khellin), efficiency increases to high values (99.3% at 300 ppm) [23].

Experimental

Inhibitors

We were the first to accomplish isolation of pure pulegone ($C_{10}H_{16}O$) from *Mentha pulegium* and preparation of pulegone oxide ($C_{10}O_2H_{16}$). For this goal the plant material was air dried at room temperature. Then it was pulverized and the essential oil was isolated after steam-distillation, using a *Clevenger* apparatus. The pure pulegone was obtained after column chromatography (silica gel, *n*-hexane) with a yield of 60% [24]. Pulegone oxide was prepared by oxidation of pulegone with *m*-chloroperbenzoic acid (*MCPBA*) in methylene chloride or hydrogen peroxide in basic media [25]. The product was identical to the one described in Ref. [25].

Weight loss measurements

Corrosion tests were carried out using coupons prepared from steel having the composition: 0.21% C, 0.38% Si, 0.09% P, 0.01% Al, 0.05% Mn, 0.05% S, and 99.21% Fe. The aggres-

Table 6 Kinetic parameters of the corrosion rate of steel in the absence and presence of *P* and *PO*

	Pre-exponential factor/ mg cm^{-2} h^{-1}	Linear regression coefficient	E_a/kJ mol^{-1}	$\frac{\Delta H_a^*}{\text{kJ mol}^{-1}}$	$\frac{\Delta S_a^*}{\text{J mol}^{-1}\,\text{K}^{-1}}$
Blank	1.26×10^{10}	0.998	83.4	56.6	−60.8
P	3.85×10^{12}	0.997	63.8	76.3	−13.1
PO	2.23×10^{11}	0.997	59.3	70.1	−36.8

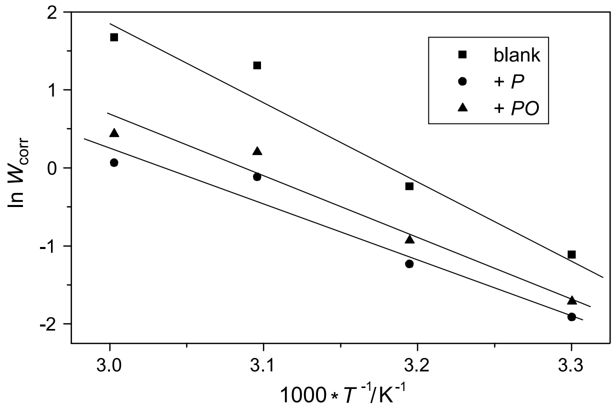

Fig. 5 *Arrhenius* plots of the corrosion rate for both the blank and the solution of inhibitor

sive solution (1 *M* HCl) was prepared by dilution of Analytical Grade 37% HCl with double distilled water.

Weight loss was measured on sheets of steel of apparent surface area of 2 cm^2. These sheets were abraded successively with fine emery paper until 1200 grade. The sheets were then rinsed with distilled water, degreased with ethanol, and dried before being weighed and immersed in 60 cm^3 of the corrosive medium. The immersion time for the weight loss was 6 h at 298 K in air without bubbling in a double-walled glass-cell equipped with a thermostat-cooling condenser. The corrosion rate was determined by hanging the steel coupon in acid solution with and without inhibitor. Each value is the mean of triplicate experiments. The inhibition effect, IE_W, for the weight loss method is calculated by:

$$IE_W = \left(1 - \frac{W_{corr}}{W^o_{corr}}\right) \cdot 100 \quad (3)$$

where W_{corr} and W^o_{corr} are the corrosion rates of steel samples with and without inhibitor.

Polarization measurement

Electrochemical measurements were carried out in a conventional three-electrode electrolysis cylindrical Pyrex glass cell. The working electrode had the form of a disc cut form steel sheet. The exposed area to the corrosive solution was 1 cm^2. A saturated calomel electrode (SCE) and a platinum electrode were used as reference and auxiliary electrodes. Running on an IBM compatible personal computer, the 352 Soft Corr^{TM} III Software communicates with an EG & G Princeton Applied Research Model 263 A potentiostat-galvanostat model 263A at a scan rate of 20 mV min^{-1}. The cell was thermostated at 298 ± 0.5 K. Before recording the cathodic polarization curves, the steel electrode was polarized at -800 mV for 10 min. For anodic curves, the potential of the electrode was swept from its corrosion potential after 30 min at free corrosion potential, to more positive values. The test solution was de-aerated with pure nitrogen. Gas bubbling was maintained through the experiments. Near E_{corr} a scan through a potential range gave polarization resistance measurements. All potentials are given in the SCE scale. For electrochemical measurements, the inhibition efficiency, IE_i, is calculated by:

$$IE_i = \left(1 - \frac{i_{corr}}{i^o_{corr}}\right) \cdot 100 \quad (4)$$

where i_{corr} and i^o_{corr} are the corrosion current density values with and without inhibitor, determined by extrapolation of cathodic *Tafel* lines to the corrosion potential.

Impedance spectroscopy measurements

Impedance spectroscopy measurements were carried out in a conventional three electrodes electrolysis cylindrical Pyrex glass cell. The working electrode had the form of a disc cut from an iron sheet. The exposed area to the corrosive solution was 1 cm^2. An SCE and a disc platinum electrode were used as reference and auxiliary electrodes. The temperature was thermostatically controlled at 298 ± 0.5 K. The electrochemical impedance spectroscopy (EIS) measurements were carried out with the electrochemical system, which included a digital potentiostat model Volta lab PGZ 100 computer at E_{corr} after immersion in solution without bubbling. After determination of steady-state current at a given potential, sine wave voltage (10 mV peak to peak), at frequencies between 100 kHz and 10 MHz was superimposed on the rest potential. Computer programs automatically controlled the measurements performed at rest potentials after 30 min of exposure. The impedance diagrams are given in the *Nyquist* representation.

The charge-transfer resistance (R_t) values are calculated from the difference in impedance at lower and higher frequencies, as suggested by *Tsuru et al.* [26]. The double-layer capacitance (C_{dl}) and the frequency at which the imaginary component of the impedance is maximal ($-Z_{max}$) are found as described by the following equation:

$$C_{dl} = (1/\omega \cdot R_t) \quad \text{where } \omega = 2\pi f_{max} \quad (5)$$

The inhibition efficiency (IE_R) got from the charge transfer resistance is calculated by:

$$IE_R = \left(1 - \frac{R_t}{R^o_t}\right) \cdot 100 \quad (6)$$

where R_t and R^o_t are the charge transfer-resistance values with and without inhibitor.

References

1. El-Etre AY (2003) Corros Sci 45:2485
2. Bouyanzer A, Hammouti B, Majidi L (2006) Mater Lett 60:2840
3. Bouyanzer A, Majidi L, Hammouti B (2006) Bull Electrochem 22:321
4. Ismail KM (2007) Electrochim Acta 52:7811
5. El-Etre AY (2007) J Colloid Interface Sci 314:578
6. Chetouani A, Hammouti B (2003) Bull Electrochem 19:23

7. Chetouani A, Hammouti B, Benkaddour M (2004) Resin Pigment Technol 33:26
8. Bendahou M, Benabdellah M, Hammouti B (2006) Pigm Resin Technol 35:95
9. Benabdellah M, Bendahou M, Hammouti B, Benkaddour M (2006) Appl Surf Sci 252:6212
10. Bouklah M, Hammouti B (2006) Port Electrochim Acta 24:457
11. Hammouti B, Kertit S, Melhaoui M (1995) Bull Electrochem 11:553
12. Bouyanzer A, Hammouti B, Majidi L (2006) Mater Lett 60:2840
13. Hall RA, Oser BL (1965) Food Technol 19:253
14. Ravid U, Putievsky E, Katzir I (1994) Flavour Fragrance J 9:205
15. Meral GE, Konyalioglu S, Ozturk B (2002) Fitoterapia 73:716
16. Mansfeld F, Kending MW, lorentz WJ (1985) J Electrochem Soc 132:290
17. Szklarska-smialowska Z (1991) Electrochemical and Optical Techniques for the study of Metallic Corrosion. Kluwer Academic Publishers, Dordrecht, p 545
18. Bard AJ, Faulkner LR (1980) Electrochemical Methods. John Wiley & Sons, NY, p 517
19. Ammar IA, El Khorafi FM (1973) Werks Korros 24:702
20. Popova A, Christov M, Raicheva S, Sokolova E (2004) Corros Sci 46:1333
21. Bouklah M, Benchat N, Aouniti A, Hammouti B, Benkaddour M, Lagrenée M, Vezin H, Bentiss F (2004) Prog Orgcoat 51:118
22. Faska Z, Majidi L, Fihi R, Bouyanzer A, Hammouti B (2007) Pigm Resin Techn 36:293
23. El-Etre AY (2006) Appl Surf Sci 252:8521
24. Majidi L, unpublished work
25. Majidi L, El idrissi M (2003) Phys Chem New 9:122
26. Tsuru T, Haruyama S, Gijutsu B (1978) J Jpn Soc Corros Eng 27:573